Journal of Innovative Optical Health Sciences
Vol. 13, No. 3 (2020) 2030009 (13 pages)

DOI: 10.1142/S1793545820300098



# Photocyanine: A novel and effective phthalocyanine-based photosensitizer for cancer treatment

Dan Chen, Meiru Song, Jinling Huang*,¶, Naishen Chen†,¶,
Jinping Xue‡,¶ and Mingdong Huang§,¶
*College of Chemistry, Fuzhou University*
*Fuzhou, Fujian 350116, P. R. China*
**jlhuang12402@126.com*
†*nschen@fzu.edu.cn*
‡*xuejinping66@fzu.edu.cn*
§*HMD_lab@fzu.edu.cn*

Received 19 November 2019
Accepted 26 March 2020
Published 23 May 2020

As one of the three key components of photodynamic therapy (PDT), photosensitizers (PSs) greatly influence the photodynamic efficiency in the treatment of tumors. Photosensitizers with tetrapyrrole structure, such as porphyrins, chlorins and phthalocyanines, have been extensively investigated for PDT and some of them have already received clinical approval. However, only a few of porphyrin-based photosensitizers are available for clinical applications, and PDT has not received wide recognition in clinical practice. In this regard, PSs remain a limiting factor. Our research focuses on the rational design of new PSs. Photocyanine, a Zinc (II) phthalocyanine (ZnPc) type photosensitizer with low dark toxicity and high single oxygen quantum yield, is one of the promising PSs candidates and currently being tested in clinical trials. Here, we present an overview on the development of Photocyanine, including its design, synthesis, purification, characterization and preclinical studies, wishing to contribute to the research of more promising PSs.

*Keywords*: Photosensitizer; photodynamic therapy; cancer; Photocyanine.

## 1. Introduction

In recent years, photodynamic therapy (PDT) has received increasing attention, as anticancer drug development remains expensive and slow with many disappointing late-stage failures.[1–3] PDT is a minimally invasive therapeutic modality which can selectively exert cytotoxic effects against malignant cells. This therapeutic procedure, the first

¶Corresponding authors.

drug/device combination approved by FDA, involves administration of a photosensitizer (PS) followed by laser irradiation at a wavelength in accordance with the absorbance band of the sensitizing agent. Both preclinical and clinical studies have revealed that PDT is curative especially in early-stage tumors and highly beneficial for inoperable cancers with negligible systemic toxicity, absence of intrinsic and acquired resistant mechanisms, and greatly reduced long-term recurrences.[1,4–6]

Light and its delivery during PDT procedure are of great importance affecting antitumor efficacy, and they are generally driven by the advances in technology of lasers and availability of light systems for photoactivation.[7] Since the optical properties of laser light make it efficient to be coupled into small optical fibers, lasers are preferred for applications in *in-vivo* light delivery. With the progress in diode technology, bulky and expensive light source in early period have gradually been displaced by relatively inexpensive and lightweight laser systems. In addition, light emitting diodes (LEDs), the nonlaser light sources, are easily portable and required much less energy to produce light with desired wavelengths, which is suitable for flat surface illumination in PDT process.[7,8]

Apart from light source, PS is another key element in PDT and the approval of new PSs for clinical application had proven extremely arduous and lengthy. Hence, much attention of medicinal chemists in this field has been focused on the development and optimization of photosensitive compounds for PDT. An ideal PS should be chemically pure, soluble and stable in pharmaceutical formulations and physiologic environment, highly photoactive and photostable, nontoxic in the dark, specifically accumulating in tumors and rapidly excreted from the body, and should have a strong absorption in phototherapeutic window (600 nm to 800 nm) and minimal absorbance between 400 nm to 600 nm.[1,9–11] The first generation of PSs, are haematoporphyrin derivatives (HpD), with Photofrin® as an acclaimed example. By now, a large number of second-generation PSs have been chemically synthesized with core structure mainly of porphyrins and chlorins,[9,12–15] among which a few with a high degree of chemical purity, low skin phototoxicity and high absorbance in the red spectral region have entered the clinical trials.

In the early 1990's, we began a systematic search for a novel phthalocyanine-based PSs with improved photochemical properties and photodynamic effect in oncology. We designed and synthesized a plethora of candidate molecules, and then screened them using both cell-based *in vitro* bioassay and mouse xenograft tumor models, and finally discovered Photocyanine (generic name: SHUTALANZIN), a mixture of four isomers of di-(potassium sulfonate)-di-phthalimidomethyl phthalocyanine zinc ($ZnPcS_2P_2$, Pc stands for phthalocyanine, S stands for sulfonate group and P stands for phthalimidomethyl group) to be the most promising phthalocyanine complex. Photocyanine has some advantages as follows: (1) the amphiphilicity of Photocyanine endows it with easy delivery in circulatory system, permeation into tumor tissue and enhanced uptake by tumor cells; (2) strong absorbance with a high extinction coefficient ($\varepsilon$) at 670 nm where tissue penetration of light is at its maximum and side effects induced by visible light are greatly reduced; (3) high quantum yield of singlet oxygen; (4) high potency, leading to comparable therapeutic efficacy to Photofrin® at a dose of 10 times less. This sensitizer was approved by CFDA for clinical trials, and are currently in phase II clinical trial on patients with esophagus cancers. In this paper, we summarize the development and the current status of Photocyanine, including its synthesis, purification, physicochemical properties, and preclinical studies.

## 2. Design of Photocyanine ($ZnPcS_2P_2$), A Phthalocyanine Derivative

The phthalocyanine (Pc) can be traced back to 1933, when Sir Reginald Linstead first coined the term to describe a class of macrocyclic compounds discovered in 1907 by Braun and Tcheriac in the synthesis of o-cyanobenzamide from phthalamide and acetic anhydride. Linstead and his group thenceforth began their comprehensive work on Pc's, leading to the determination of the structure of Pc's via X-ray crystallography and the formation of several metallo-Pc complexes (MPc's) in the early 1930s.[16]

The photodynamic effect of antitumor PSs mainly depends on their photosensitivity and uptake into tumor cells. Photosensitivity is generally determined by the quantum yield of singlet oxygen produced when the photosensitizer interacts with surrounding oxygen. The uptake of PSs into tumor

cells and tissue correlates with their electric charge characteristics, hydrophilicity/hydrophobicity balance, and geometrical configuration of the substituents.[17] There were extensive studies on the photodynamic properties of MPc's with variations in the nature of the central metal ion and the peripheral substituents. Under illumination at appropriate wavelengths, PSs are excited from singlet ground state ($S_0$) to the first excited singlet state ($S_1$), and then switched to the triplet state ($T_1$) through intersystem crossing (ISC), which directly determines their photosensitivity. Heavy metal occupancy at Pc is known to enhance ISC. Typically, diamagnetic metals promote ISC and have a long triplet lifetime, while paramagnetic metals deactivate excited states, reduce the excited-state lifetime and prevent photodynamic process. In our studies, the ability of a series of MPcs to produce $^1O_2$ is as follows: ZnPc > AlClPc ≫ CrPc > MnPc > CoPc > NiPc > FeClPc > FePc.[18] Meanwhile, the unsubstituted MPc aggregate readily in the solution due to its poor water solubility. Polymeric species not only show a decrease in fluorescence emission due to self-quenching, but also impede *in vivo* transportation. Therefore, peripheral substituents are often introduced to MPc to improve hydrophilicity and reduce aggregation propensity. The balance between the hydrophilicity and hydrophobicity of a PS is critical for its efficacy, since hydrophilicity benefits *in vivo* transport and hydrophobicity benefits tumor cell uptake. It has been shown that *cis*-disulfonated phthalocyanine complexes (bisulfonic acid groups are located on two adjacent benzene rings) are amphiphilic and capable of cell membrane penetration, thus increasing potency to induce direct cell killing during PDT.[19] Margaron *et al.* synthesized a series of $MPcS_nPh_m$, where S stands for sulphonate group and Ph stands for phenyl group, and the results indicated that photoactivity of $ZnPcS_nPh_m$ was maximized when $n = m = 2$ with a $LD_{90}$ of 3.75 $\mu$M in V79 Chinese hamster lung cells. However, photoactivity of $MPcS_2Ph_2$ did not surpass $MPcS_2$ due to reduced photosensitivity.[20] Paquette *et al.* studied the structure–activity relationship of $Al(OH)PcS_nP_m$, where S stands for sulphonate group and P stands for phthalimidomethyl group. They found that the change in $n/m$ did not significantly affect the photosensitivity of $Al(OH)PcS_nP_m$, but the lipophilicity of the complexes increased with more phthalimidomethyl groups, thus improving tumor cell uptake as well as photoactivity both *in vitro* and *in vivo*.[21] These results indicated that tumor cells appeared to have strong affinity for phthalimidomethyl group, presumably due to the overexpressed low-density lipoproteins on the tumor cells. Our research team focused on $ZnPcS_nP_m$, and found that amphiphilic $ZnPcS_2P_2$ displayed superior photodynamic activity with a survival fraction of 55.84% in HL60 cells (treated with 1 $\mu$g/mL of $ZnPcS_2P_2$) and a tumor inhibition rate of 90.8% in U14 cervical carcinoma bearing mice (drug dosage: 2 mg/kg, light dose: 72 J/cm$^2$).[22]

## 3. Synthesis and Purification of Photocyanine

Throughout the history of the development of Pc-based photosensitizer, the synthesis of unsymmetrically substituted MPc with high yield and high purity remained a major challenge. Statistical condensation is a conventional method to build phthalocyanine ring, but the products are typically mixture of numerous isomers. Mono-and disubstituted lipophilic MPcs and their analogues can be prepared via statistical condensation of an iminoisoindoline derivative with either a 1,3-bis[(3′-imino-1′-isoindolinydene)amino]-1,2,4-triazole or a 1,3,3-trichloroisoindoline.[23–25] However, such method has not been used in the synthesis of MPc containing hydrophilic substituents. Kudredich *et al.* reported the synthesis of ZnPc substituted with one sulfonate group and three tertiary butyl groups via statistical condensation of 4-nitrophtalonitrile and 4-tert-butylphthalonitrile followed by sulfonation. Later, they developed a novel strategy to synthesize trisulfonated ZnPc ($ZnPcS_3$) by ring expansion of boron tri(4-sulfo) subphthalocyanine (trisulfo-SubPcB(OH)), which was prepared by hydrolysis of tri(4-chlorosulfonyl)SubPcB(Br) obtained from condensation of 4-(chlorosulfonyl)phthalonitrile with $BBr_3$ in chlorobenzene.[26] Yet, our disulfonated ZnPc cannot be prepared via this route. In our early studies, amphiphilic $ZnPcS_2P_2$ was synthesized by a simple one-pot reaction starting from unsubstituted ZnPc, phthalimide, poly-formaldehyde and fuming sulfuric acid in concentrated sulfuric acid; however, the complex mixture obtained in this method required time-consuming chromatographical separations, and the yields of $ZnPcS_2P_2$ was far from satisfactory. It was noteworthy that Nolan *et al.*

reported the preparation of 2,3,9,10-tetrakis(3,3-dimethyl-1-butynyl)phthalocyanine and 2,3,9,10-tetramethoxy–phthalocyanine via condensation of a "half" phthalocyanine intermediate (obtained from 4,5-bis(3,3-dimethyl-1-butynyl)phthalonitrile or phthalonitrile) with phthalonitrile and 4,5-dimethoxy–phthalonitrile, respectively.[27]

We developed a novel method to synthesize sulfonate and phthalimidomethyl ZnPc with high yield and successfully filed a patent (ZL 200410013492.4). In our method, potassium 4-sulfophthalonitrile and 4-phthalimidomethyl phthalonitrile were used as starting materials to synthesize two precursors, i.e., disulfonated "half" phthalocyanine intermediate and disphthalimidomethylated "half" phthalocyanine intermediate, which were then cyclized in 2-methoxyethanol with molar ratio of 1:0.8–1.2, and finally metalation was achieved by adding anhydrous zinc acetate in DMF in the temperature range of 120°C to 200°C (Scheme 1).

The reaction product is a mixture of $ZnPcS_nP_{4-n}$ ($n = 0 - 4$), with the two substituted groups located on either opposite or adjacent benzene rings and the isoindole rings exhibiting two beta substitution sites. Based on statistical distribution, ratio distribution of possible isomers is predicted. In comparison of different analytical methods for separating sulfonated Pc derivatives, van Lier *et al.* found that reversed-phase-HPLC (rp-HPLC) with gradient elution was optimal by using methanol and phosphate buffer as mobile phase. In this way, they successfully separated $GaPcS_nCl$, the Pc derivatives containing different number of sulfonate groups.[28] The Pc derivatives with more sulfonate groups would be eluted preferentially in reverse-phase HPLC column and that the isomer with disperser sulfonate groups (*trans*-isomers) would be eluted faster. Based on these results, we separated $ZnPcS_2P_2$ out from $ZnPcS_nP_{4-n}$ ($n = 0 - 4$) mixture by gradient elution with solution A of 10 mM trimethylamine (TEA) in 5 mM phosphate buffer (pH 7.0) and solution B of DMF. $ZnPcS_nP_{4-n}$ gave five characteristic groups of peaks in this separation, which were assigned as $ZnPcS_4$, $ZnPcS_3P$, $ZnPcS_2P_2$, $ZnPcSP_3$, $ZnPcP_4$ (Fig. S1).[29] $ZnPcS_2P_2$ was eluted at the third group with a retention time of 21.0–21.8 min. $ZnPcS_2P_2$ consists of five *trans*-isomers and 10 *cis*-isomers according to statistical distribution (Fig. S2). Although these $ZnPcS_2P_2$ isomers have similar photophysics and photochemistry characteristics, their pharmacological properties may vary with selectivity in organism localization and uptake. By comparing the two chromatogram curves obtained with water/DMF or phosphate buffer/DMF as eluent, we found that the retention of $ZnPcP_4$ remained unchanged while $ZnPcS_4$ was eluted as one broad early peak in water/DMF, indicating that sulfonate group has a major effect on retention time. Besides, a comparison of chromatogram profiles of $ZnPcS_3P$ and $ZnPcSP_3$ showed that $ZnPcS_3P$ gave a group of three peaks while $ZnPcSP_3$ gave an overlap peak (Fig. S3). It appears that sulfonate groups rendered better peak separation of isomers for the isomers with the same number of sulfonate groups. In order to assign this HPLC profile to structural isomers of $ZnPcS_2P_2$, we firstly identified the isomers of $ZnPcS_2$. According to statistical distribution of condensation reaction, there are two *cis*-isomers and three *trans*-isomers of $ZnPcS_2$. Our results showed clear baseline separation of all these five isomers, which were assigned in reference of the

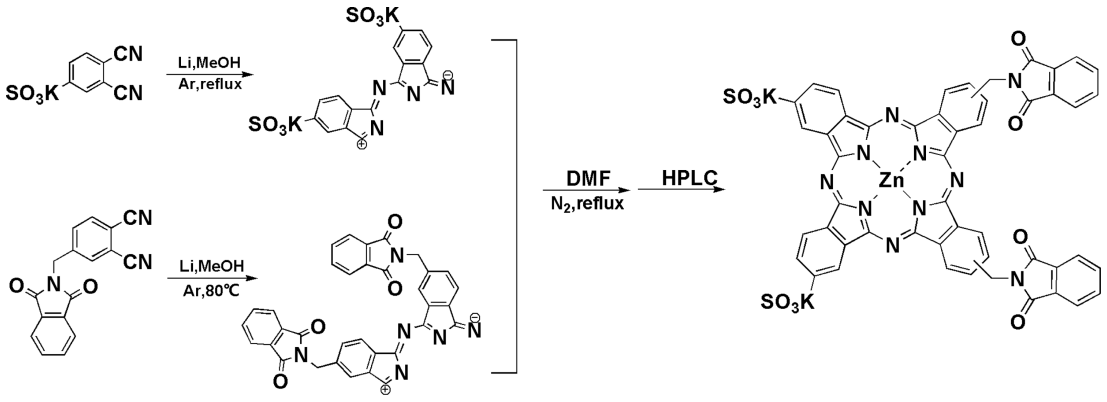


Scheme 1. The synthesis of Photocyanine.

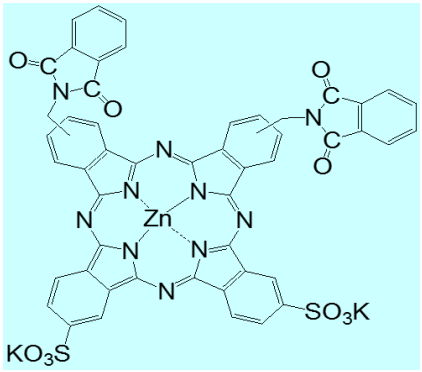


(a)

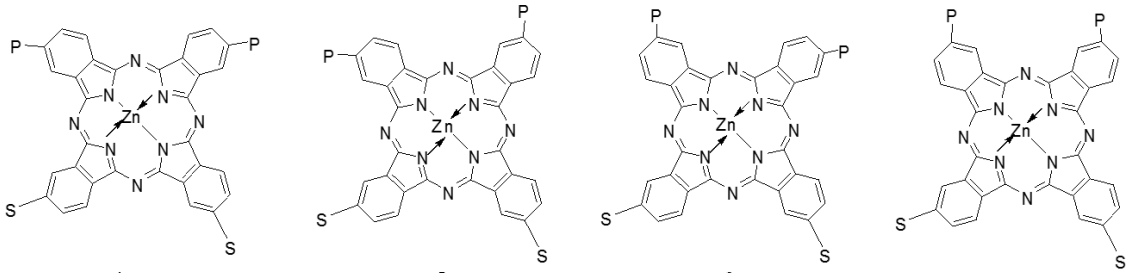


(b)

Fig. 1. (a) Chemical structure of Photocyanine; (b) explicit isomer composition of Photocyanine.

previous data by van Lier group (Fig. S4). It appears that *trans*-isomers (SPSP type), in which the sulfonate groups are located oppositely to each other, are more hydrophilic than *cis*-isomers (SSPP type), in which the sulfonate groups are located closely to each other, resulting in faster elution of *trans*-isomers than that of *cis*-isomers. Similar to $ZnPcS_2$, the elution profile of $ZnPcS_2P_2$ also follow this rule. We then successively separated *cis*-isomers and *trans*-isomers of $ZnPcS_2P_2$ sample on preparative HPLC through isocratic elution and gradient elution, respectively (Figs. S5 and S6).[29] Furthermore, the structures of $ZnPcS_2P_2$ isomers were confirmed using NMR method. For drug

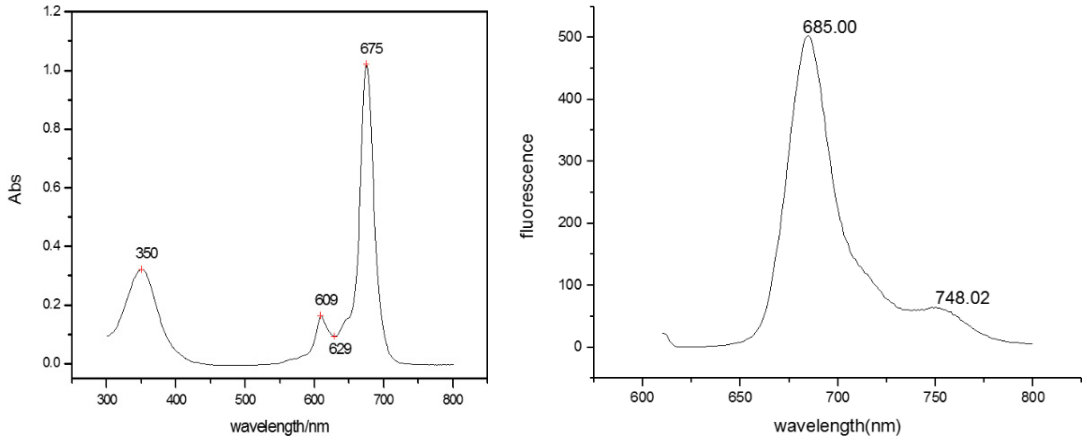


(a) (b)

Fig. 2. (a) Absorption and (b) fluorescence spectra of Photocyanine in DMF.

quality control, a mixture of four isomers (4–7), with disulfonate groups and diphthalimidomethyl groups arranged in a *cis* position facilitating formation of the hydrogen bond between $ZnPcS_2P_2$ and lipoproteins on the surface of tumor cells, was prepared as Photocyanine (generic name: suftalan zinc) (Fig. 1). The structure of Photocyanine was further confirmed by $^1$H NMR and mass spectrometry (Fig. S7 and Table S1).

The photophysical properties of Photocyanine were then studied. Photocyanine has a strong absorption in the near-infrared region ($\lambda_{max} = 675$ nm in DMF), high molar extinction coefficient ($\varepsilon_{max} = 2.601 \times 10^5\,L \cdot mol^{-1} \cdot cm^{-1}$), high fluorescence quantum yield ($\Phi_F = 0.26$) and high $^1O_2$ quantum yield ($\Phi_\Delta = 0.53$) (Fig. 2).

## 4. Preclinical Study

### 4.1. *Pharmacokinetics and pharmacodynamics (PK/PD) of photocyanine*

Pharmacokinetic parameters and distribution of Photocyanine were assessed in tumor-bearing mice. S180 sarcoma cells ($10^7$ cells/200 $\mu$L) were subcutaneously implanted in the right axillary region of Kunming mice (half male and half female) aged 4–6 weeks and weighing 18–22 g. Mice were intravenously administered a single dose of Photocyanine (2 mg/kg) formulated in saline containing 2% Cremophor EL and 20% 1, 2-propylene glycol when tumors reached an approximate size of 5 mm in diameter. The mean serum concentrations of Photocyanine declined in a manner best fitted by a two-compartment open model with distribution phase half-lives of 2.77 h and 2.66 h for male and female mice, respectively, and elimination phase half-lives of 34.07 h and 41.33 h for male and female mice, respectively. Peak serum concentrations of Photocyanine were $10480 \pm 628$ and $9438 \pm 547$ ng/mL in male and female mice, respectively. The area under the serum concentration versus time curve (AUC) were $79.51\,mg \cdot mL^{-1} \cdot h$ and $57.8\,mg \cdot mL^{-1} \cdot h$ in male and female mice, respectively (Fig. 3). After *i.v.* administration, Photocyanine was widely distributed to tissues. Of the tissues examined, the highest level of Photocyanine was demonstrable in the liver, which peaked at 72 h and then decreased gradually. The concentration of Photocyanine in tumor was lower than that in liver, intestine, testis and ovary tissues. Peak Photocyanine concentration in the tumor occurred at 6 h, and sustained above 500 ng/g until 72 h. The content of Photocyanine in the skin peaked at 24 h, then decreased gradually. And there was still a certain amount of Photocyanine accumulating in the skin on the 21st day. The distribution of Photocyanine in other tissues was much lower than those mentioned above, and the order from high to low was skin, spleen, lung, kidney, heart, stomach, bladder and fat. In addition, Photocyanine was barely distributed in the brain, muscle and eyeball (Fig. 4). The results showed that the effect of gender on pharmacokinetics and tissue distribution of Photocyanine was not obvious. These results were further validated using a [$^{14}$C]Photocyanine in male Sprague-Dawley (SD) rats.

The *in vitro* photodynamic activity of Photocyanine against a variety of tumor cells was

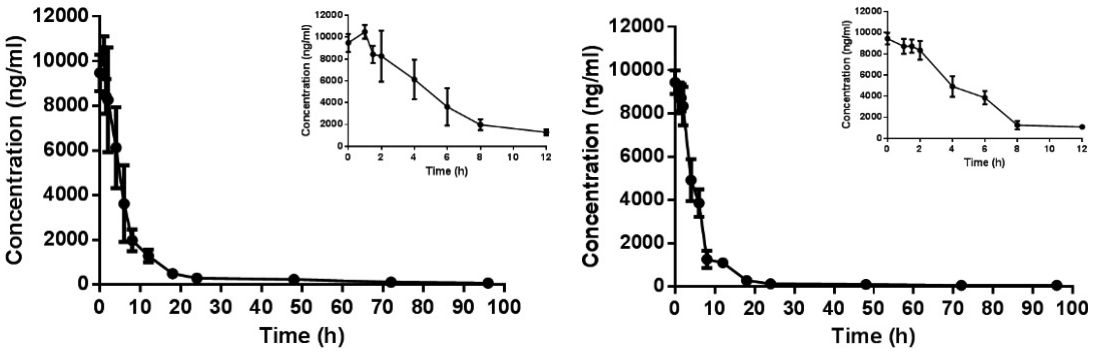


(a) (b)

Fig. 3. Mean concentration–time profile of Photocyanine in serum of male (a) and female (b) Kunming mice bearing S180 tumors ($n = 5$).

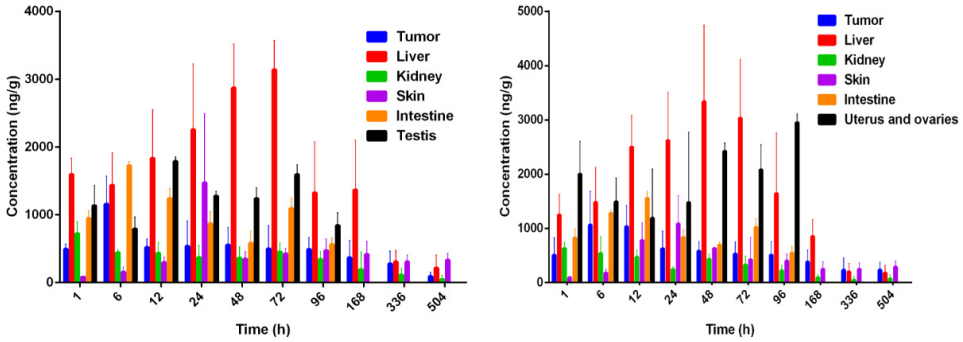


Fig. 4. Distribution of Photocyanine in various tissues of male (a) and female (b) Kunming mice bearing S180 tumors ($n = 5$).

characterized before *in vivo* evaluation with tumor xenografts was undertaken. It was shown that Photocyanine significantly inhibited the growth of more than 10 kinds of tumor cells, including human gastric cancer, colon cancer, liver cancer, lung cancer, glioma, oral cancer, renal cancer, ovarian cancer, melanoma, prostate cancer, esophagus cancer and skin cancer, with corresponding $IC_{50}$ values well lower than those of HpD, exerting pronounced *in vitro* photosensitive killing activity (Table 1). When injected with Photocyanine at a dose of 2 mg/kg, the growth inhibition rates of cervical carcinoma U14, sarcoma S180 and liver cancer H22 xenografts reached approximate 60%, 70% and more than 70%, respectively. Additionally, the inhibition rate of tumor growth in human colon carcinoma COLO 205-bearing nude mice was 70% and the relative tumor proliferation rate T/C (%) was lower than 50% after treatment with 2 mg/kg of Photocyanine. Furthermore, according to our results, the inhibitory effect of Photocyanine (dose: 2 mg/kg, irradiation under 670 nm) on tumor xenograft growth was comparable to that of HpD (dose: 50 mg/kg) and that of Photofrin (dose: 20 mg/kg) under 630 nm irradiation.

Table 1. *In vitro* photodynamic activity of Photocyanine against various tumor cells compared with HpD.

| | $IC_{50}$ ($\mu$g/mL) | |
|---|---|---|
| | HpD | Photocyanine |
| KB | $4.589 \pm 0.3518$ | $0.058 \pm 0.0012$ |
| M14 | $4.136 \pm 0.3270$ | $0.062 \pm 0.0006$ |
| MV3 | $3.072 \pm 0.0533$ | $0.062 \pm 0.0185$ |
| BGC-803 | $3.345 \pm 0.2192$ | $0.069 \pm 0.0012$ |
| A2780 | $2.754 \pm 0.3822$ | $0.075 \pm 0.0121$ |
| Ketr-3 | $3.030 \pm 0.2119$ | $0.075 \pm 0.0142$ |
| SMMC-7721 | $3.935 \pm 0.1926$ | $0.079 \pm 0.0144$ |
| CaEs-17 | $4.241 \pm 0.4249$ | $0.069 \pm 0.0036$ |
| A431 | $3.667 \pm 0.1285$ | $0.073 \pm 0.0075$ |
| HCT-8 | $2.964 \pm 0.2723$ | $0.143 \pm 0.0806$ |
| TJ905 | $4.266 \pm 0.5376$ | $0.321 \pm 0.0969$ |
| Pc-3M | $3.413 \pm 0.2541$ | $0.361 \pm 0.1586$ |
| A549 | $3.362 \pm 0.0517$ | $0.380 \pm 0.0418$ |
| Bel 7402 | $3.308 \pm 0.0925$ | $0.414 \pm 0.0476$ |

## 4.2. *Mechanistic study*

The absorption of light leads to the activation of PS to unstable $S_1$ state, which may undergo an ISC to form a more stable $T_1$ state. The PS, in its reactive $T_1$ state, can react with biomolecules by electron transfer to form radicals (type I reaction) and/or react directly with molecular oxygen by energy transfer to generate singlet oxygen (type II reaction), which results in apoptosis and/or necrosis of exposed cells. It is commonly believed that most PSs exert cytotoxic effects via type II instead of type I mechanism, since reactive oxygen species (ROS) generation via type II photochemical process is theoretically much simpler than via type I.[1,6] However, an increasing number of studies have shown that PSs still possess satisfactory antitumor effect under hypoxic condition, demonstrating the importance of overlooked type I pathway.[30–32] Due to the short half-life and diffusion distance of singlet oxygen ($^1O_2$) and most radicals, intracellular location of the PSs is crucial to induce photodynamic damage during PDT.[33,34] During preclinical research, researchers in our group explored the molecular mechanisms of Photocyanine on human hepatocellular carcinoma (HepG2) cells to guide further drug development.[35,36] The amphipathic Photocyanine was found to permeate through the

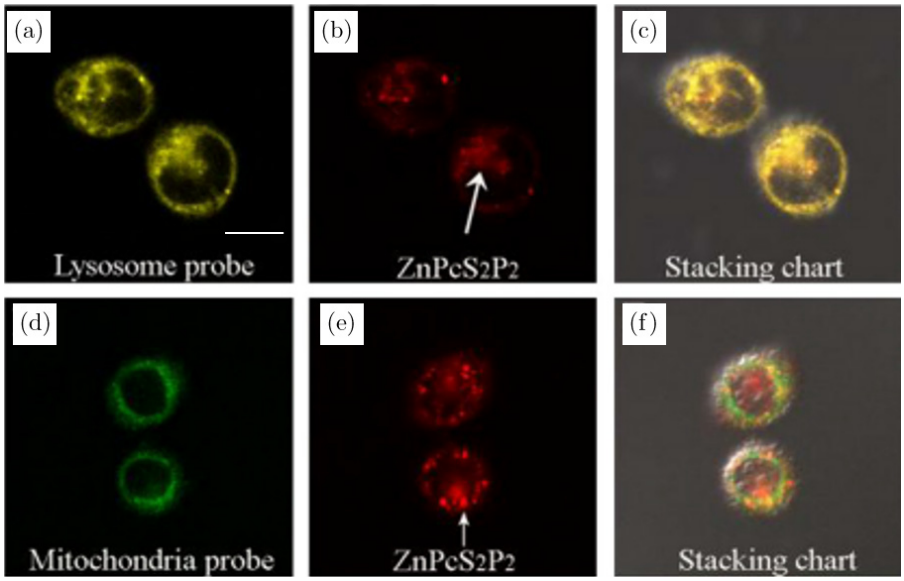


Fig. 5. Intracellular distribution of Photocyanine in HepG2 without irradiation. Lysosome (a) and mitochondria (d) were stained with LysoTracker Red (emitted at 577 nm) and Mito-Tracker Green (emitted at 490 nm), respectively. (b) and (e) showed intracellular Photocyanine accumulation (10 $\mu$M) detected by red fluorescence. (c) and (f) showed stacked pictures of the red granular Photocyanine particles with yellow lysosome (c) and green mitochondria (f), respectively (original magnification $\times$ 60, bar = 20 $\mu$m). Reproduced with permission from Ref. 35.

cell membrane of HepG2, predominately locate to lysosome and mitochondria, and to a lesser extent, concentrate in cytoplasm and on nuclear membrane. Nevertheless, Photocyanine was not capable of penetrating through the nuclear membrane (Fig. 5). The exposure of HepG2 cells to Photocyanine with light irradiation resulted in concentration-dependent decrease of mitochondrial membrane potential ($\Delta\psi$m) and increase of caspase-3 activity, revealing the apoptotic effect by Photocyanine on HepG2 (Fig. 6). In addition, ROS generation was prominent and concentration-dependent induction of apoptosis or necrosis following Photocyanine incubation and irradiation was also observed (Figs. 7 and 8). Cell death pathways were further analyzed by acridine orange/ethidium bromide (AO/EB) staining. The fluorescent phase-contrast images showed that HepG2 cells displayed distinct nucleolus pyknosis and congregated chromatin, a phenomenon of early apoptosis, at a Photocyanine concentration of 2.5 $\mu$M. With the increase of Photocyanine concentration to

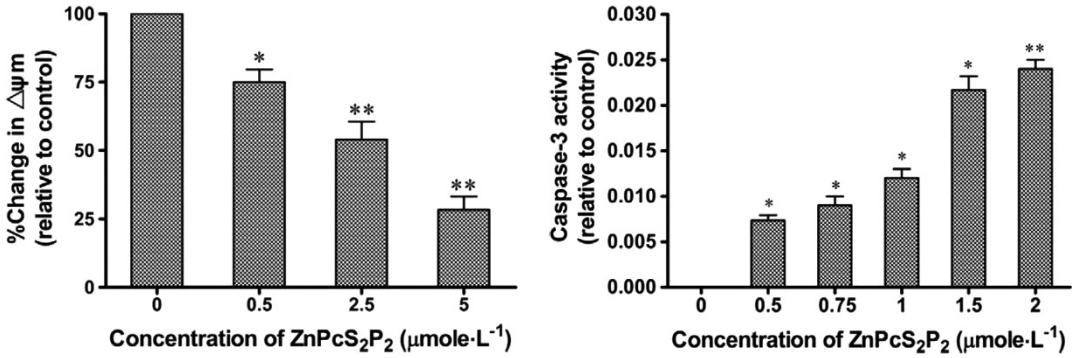


(a) (b)

Fig. 6. Effects of Photocyanine on mitochondrial membrane potential ($\Delta\psi$m) (a) and caspase-3 activity (b) of HepG2 Cells. Statistical difference from controls: $^*P < 0.05$; $^{**}P < 0.01$ ($n = 6$). Reproduced with permission from Ref. 35.

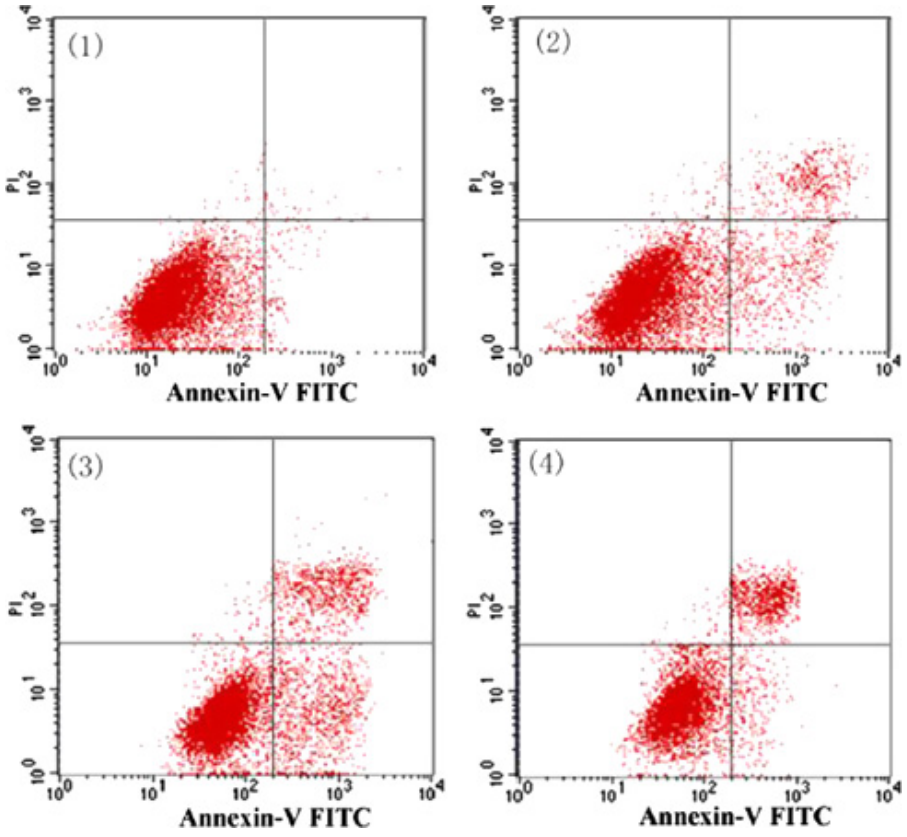


(a)

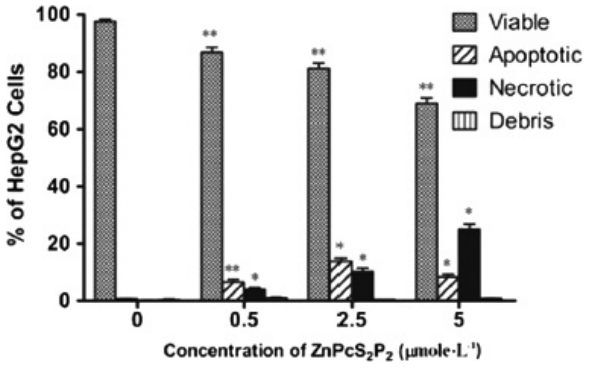


(b)

Fig. 7. Annexin V-EGFP/PI cell apoptosis detection by flow cytometry of HepG2 treated with Photocyanine plus irradiation. The cells were left untreated (A1), or treated with 0.5 (A2), 2.5 (A3), or 5 (A4) $\mu$M of Photocyanine plus irradiation. There were three populations of cells: viable, apoptotic (Annexin V-EGFP positive and PI negative), and necrosis or in late stage of apoptosis (Annexin V-EGFP and PI positive). Panel b showed concentration-dependent induction of apoptosis or necrosis by Photocyanine. The upper left quadrant of panel a represented a portion of damaged cells (debris, in panel b) that occurred in the process of the cells. $^{*}P < 0.05$ and $^{**}P < 0.01$ compared with the untreated controls. Reproduced with permission from Ref. 35.

5 $\mu$M, the cells demonstrated nuclear fragmentation and apoptotic bodies formation, a phenomenon of a late apoptotic stage, as well as cell membrane ruptures and the weaken of yellowish green fluorescence, a phenomenon of necrosis (Fig. 9).

### 4.3. *Tumor specificity*

Intravenously administered PSs firstly bind to various serum proteins while circulating in blood, then gradually escape vasculature and penetrate to tumor tissue. The effect of PDT against tumors

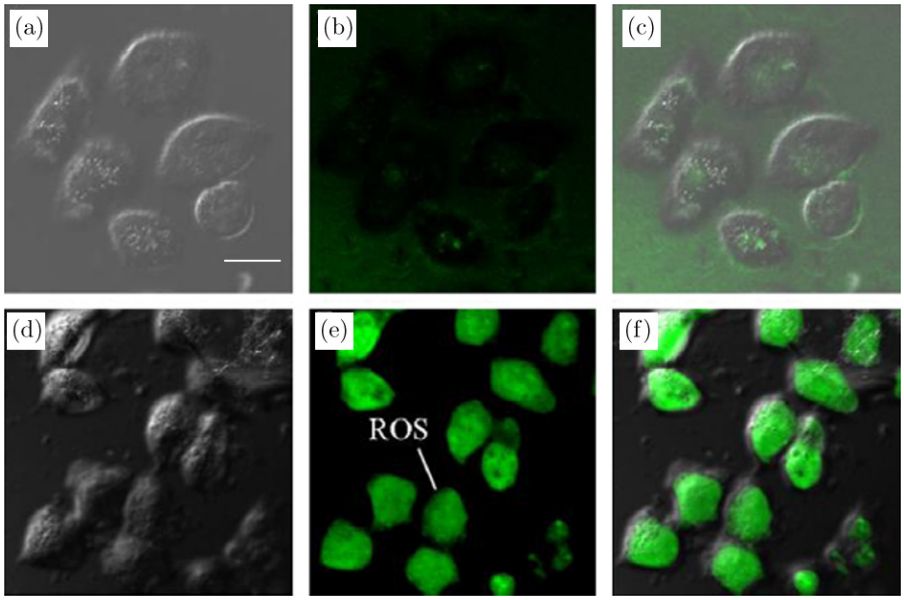


Fig. 8. ROS production in HepG2 cells treated with 0.5 $\mu$M Photocyanine and irradiation (the lower panels) compared with that of untreated cells (the upper panels). (a) and (d) — bright field; (b) and (e) — fluorescent images in the presence of ROS probe; (c) and (f) — the merged images (original magnification $\times 60$, bar = 20 $\mu$m). Reproduced with permission from Ref. 35.

depends on at which stage of this sequent process light is delivered.[37–39] Therefore, defining the profile of PSs distribution in the tumor compared with that in the peritumoral normal tissue is highly desired to maximize the therapeutic effect as well as to minimize the side effects of PDT. We utilized a noninvasive method to determine the tumor-to-peritumoral tissue drug concentration ratio (CR) by *in vivo* three-dimensional optical imaging. BALB/c nude mice bearing EC109 tumors were *i.v.* injected with Photocyanine preparation (25 nM) and imaged by a Fluorescence Molecular Tomography (FMT) imaging system (PerkinElmer FMT-2500 LX), which allows 3D and quantitative imaging. Regions of interest (ROIs) were selected in tumor and peritumoral tissue, respectively. Selection criteria: $ROI_{tumor}$ was in the tumor tissue where the fluorescence was strongest within 3 mm depth from body surface; and $ROI_{normal}$ was in peritumoral normal tissue where the fluorescence was strongest within 3 mm depth from body surface and 5 mm width from tumor tissue boundary. CR was calculated as $C_{tumor}/C_{normal}$ in the corresponding ROIs, which reached 3.03 to 3.83 between 1 h to 6 h post dosing, maintained around 2.7 between 8 h to 12 h post dosing and was still larger than 1 after 48 h (Fig. 10). The advantages of 3D and quantitative *in vivo* imaging technology, such as noninvasiveness and high sensitivity, reduced the drug dosage (0.28 mg/kg needed with FMT versus 2 mg/kg needed with fluorescence spectrophotometry) as well as the number of animals required for the experiment, greatly facilitating the early evaluation of

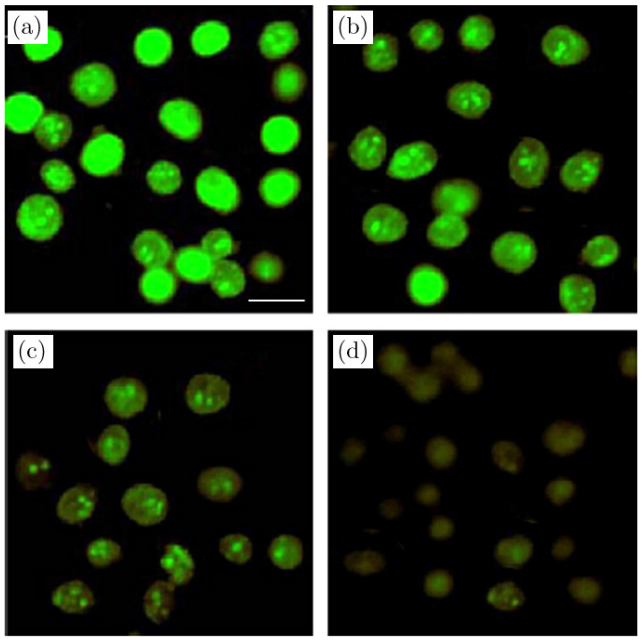


Fig. 9. Composite images of acridine orange/ethidium bromide (AO/EB) stained HepG2 cells. (a) control; (b), (c) and (d) — treatment with 0.5, 2.5 and 5 $\mu$M Photocyanine, respectively (original magnification $\times 60$, bar = 20 $\mu$m, AO: green, EB: brown). Reproduced with permission from Ref. 35.

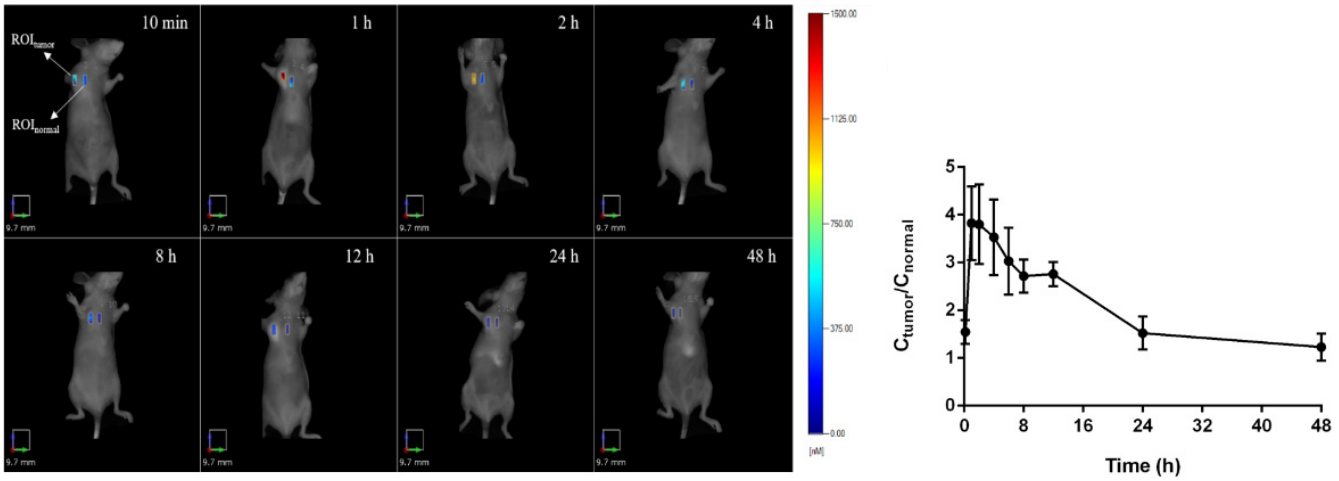


(a) (b)

Fig. 10. Tumor specificity of Photocyanine in BALB/c nude mice bearing EC 109 tumors. (a) *in vivo* 3D optical imaging at predetermined time points; (b) Photocyanine concentration ratio (CR) in the corresponding ROIs ($n = 5$).

promising PSs. The result showed that the time-window during PDT was long enough to obtain enhanced *in vivo* tumoricidal effect and decreased off-target toxicity.

### 4.4. *Toxicology*

A dose escalation study was performed in Kunming mice to evaluate the acute toxicity of Photocyanine. The $LD_{50}$ of *i.p.* injection was determined to be 51.57 mg/kg (95% CI, 35.68 mg/kg to 65.05), and the $LD_{50}$ of *i.v.* injection was 49.98 mg/kg (95% CI, 39.86 mg/kg to 63.05). A repeated-dose study of Photocyanine-based PDT was conducted in beagle dogs to determine its chronic toxicity. 24 dogs were divided into four groups randomly, and administered Photocyanine preparation intravenously at doses of 0, 0.5, 1.5 and 4.5 mg/kg, followed by irradiation with 670 nm laser in 48 h and 72 h post dosing. This dosage regimen was successively performed once every four days for 10 times. A majority of dogs experienced dysphoria and a few had slight edema on the faces after Photocyanine *i.v.* administration. No mortality or abnormity in electrocardiography, ophthalmoscopy, hematology and urinalysis were observed. Histologic examination showed hepatic spotty and lytic necrosis in the group dosed at 4.5 mg/kg (equivalent to 45 times of the intended dose in human), which was alleviated at the end of observation period. And the dose of 1.5 mg/kg was regarded as the NOAEL.[40]

In addition, no obvious phototoxicity was observed in Kunming mice even when the dose of Photocyanine was as high as 5 mg/kg. Systemic administration of Photocyanine did not cause allergic effect and hemolytic phenomena in guinea pigs and rabbits. Vascular stimulation at the injection site was investigated in rabbits' ear vein, and microscopic examination showed local irradiation to the blood vessel wall damaged by puncture, which disappeared 2 cm from the injection site. Detection of Photocyanine as mutagens in the salmonella/microsome test and chromosomal aberration test showed no gene mutation in all four salmonella strains, no micronucleus formation in the bone marrow erythrocytes of Kunming mice, and no increase of chromosome aberration rate in Chinese hamster lung cells (CHL) within the concentration range of 50 $\mu$g/mL to 400 $\mu$g/mL.

## 5. Conclusion and Perspective

PDT has been around for over a century and has been used as an effective treatment modality for the past two decades. However, this therapy modality is not widely used in clinical practice due to, for one reason, limited availability of clinical PSs, which is a key component of PDT. Most of the PSs now are based on porphyrin or its analogue. We report here the development process of a new PS, Photocyanine, which is based on another type of PS, zinc phthalocyanine, and represents the first of this class entering clinical trials. Despite the long history and

process in obtaining Photocyanine, the Phase I clinical trial showed not only the safety but also overall positive outcome for cancer patients. Photocyanine has been considered to be a promising PS candidate in PDT for cancer and undergone a phase II clinical trial in patients with primary esophageal carcinoma. This work opens up a new avenue for the development of new type of PSs.

## Conflict of Interest

The authors declare no conflict of interest. Prof. Jinling Huang, Naisheng Chen, and Jinping Xue are the inventors of the Photocyanine.

## Acknowledgments

Our research work is financially supported by grants from National Key R&D Program of China (2017YFE0103200), National Science and Technology Major Projects for "Major New Drugs Innovation and Development" (Grant number 2011ZX09101-001-04), Natural Science Foundation of China (31370737, 31670739).

## References

1. P. Agostinis, K. Berg, K. A. Cengel, T. H. Foster, A. W. Girotti, S. O. Gollnick, S. M. Hahn, M. R. Hamblin, A. Juzeniene, D. Kessel, M. Korbelik, J. Moan, P. Mroz, D. Nowis, J. Piette, B. C. Wilson, J. Golab, "Photodynamic therapy of cancer: an update," *CA Cancer J. Clin.* **61**(4), 250–281 (2011).
2. W. N. Hait, "Anticancer drug development: The grand challenges," *Nat. Rev. Drug Discov.* **9**(4), 253–254 (2010).
3. C. Hopper, "Photodynamic therapy: A clinical reality in the treatment of cancer," *Lancet Oncol.* **1**, 212–219 (2000).
4. Z. Huang, "A review of progress in clinical photodynamic therapy," *Technol. Cancer Res. Treat.* **4**(3), 283–293 (2005).
5. N. Nishiyama, Y. Morimoto, W. D. Jang, K. Kataoka, "Design and development of dendrimer photosensitizer-incorporated polymeric micelles for enhanced photodynamic therapy," *Adv. Drug Deliv. Rev.* **61**(4), 327–338 (2009).
6. M. Ethirajan, Y. H. Chen, P. Joshi, R. K. Pandey, "The role of porphyrin chemistry in tumor imaging and photodynamic therapy," *Chem. Soc. Rev.* **40**(1), 340–362 (2011).
7. T. S. Mang, "Lasers and light sources for PDT: Past, present and future," *Photodiagn. Photodyn. Ther.* **1**(1), 43–48 (2004).
8. L. Brancaleon, H. Moseley, "Laser and non-laser light sources for photodynamic therapy," *Lasers Med. Sci.* **17**(3), 173–186 (2002).
9. Z. Jiang, J. W. Shao, T. T. Yang, J. Wang, L. Jia, "Pharmaceutical development, composition and quantitative analysis of phthalocyanine as the photo sensitizer for cancer photodynamic therapy," *J. Pharm. Biomed. Anal.* **87**, 98–104 (2014).
10. M. Lismont, L. Dreesen, S. Wuttke, "Metal-organic framework nanoparticles in photodynamic therapy: Current status and perspectives," *Adv. Funct. Mater.* **27**(14), 1606314 (2017).
11. W. M. Sharman, C. M. Allen, J. E. van Lier, "Photodynamic therapeutics: Basic principles and clinical applications," *Drug Disc. Today* **4**(11), 507–517 (1999).
12. R. Bonnett, "Photosensitizers of the Porphyrin and Phthalocyanine Series for Photodynamic Therapy," *Chem. Soc. Rev.* **24**(1), 19–33 (1995).
13. M. O. Senge, J. C. Brandt, "Temoporfin (Foscan (R), 5,10,15,20-Tetra(m-hydroxyphenyl)chlorin)-A Second-generation Photosensitizer," *Photochem. Photobiol.* **87**(6), 1240–1296 (2011).
14. A. E. O'Connor, W. M. Gallagher, A. T. Byrne, "Porphyrin and Nonporphyrin Photosensitizers in Oncology: Preclinical and clinical advances in photodynamic therapy," *Photochem. Photobiol.* **85**(5), 1053–1074 (2009).
15. S. B. Brown, E. A. Brown, I. Walker, "The present and future role of photodynamic therapy in cancer treatment," *Lancet Oncol.* **5**(8), 497–508 (2004).
16. C. C. Leznoff, A. B. P. Lever, *Phthalocyanines: Properties and Applications*, Vol. 1, VCH (1989).
17. B. W. Henderson, T. J. Dougherty, "How does photodynamic therapy work?" *Photochem. Photobiol.* **55**(1), 145–157 (1992).
18. J. L. Huang, J. D. Huang, E. S. Liu, N. S. Chen, "Some relationships between structures and photodynamic anti-cancer activities of phthalocyanines," *Acta Phys. Chim. Sin.* **17**(7), 662–671 (2001).
19. A. R. Morgan, "Strategies for the development of photodynamic sensitizers," *Curr. Med. Chem.* **2**(2), 604–615 (1995).
20. P. Margaron, R. Langlois, J. E. Vanlier, S. Gaspard, "Photodynamic properties of naphthosulfobenzoporphyrazines, novel asymmetric, amphiphilic phthalocyanine derivatives," *J. Photochem. Photobiol. B-Biol.* **14**(3), 187–199 (1992).
21. B. Paquette, R. W. Boyle, H. Ali, A. H. MacLennan, T. G. Truscott, J. E. van Lier, "Sulfonated phthalimidomethyl aluminum phthalocyanine: The effect of hydrophobic substituents on the in vitro

phototoxicity of phthalocyanines," *Photochem. Photobiol.* **53**(3), 323–327 (1991).
22. J. L. Huang, N. S. Chen, J. D. Huang *et al.*, "Metal phthalocyanine as photosensitizer for photodynamic therapy (PDT)-Preparation, characterization and anticancer activities of an amphiphilic phthalocyanine $ZnPcS_2P_2$," *Sci. China Ser. B, Chem.* **43**(6), 481–488 (2000).
23. B. Cabezon, S. Rodriguezmorgade, T. Torres, "Stepwise synthesis of soluble substituted triazolephthalocyanines," *J. Org. Chem.* **60**(6), 1872–1874 (1995).
24. J. Yang, T. C. Rogers, M. R. Vandemark, "Synthesis of 1,2,3,4-Tetraphenyl-9,10,16,17,23,24,-Hexadodecyloxyphthalocyanine," *J. Heterocyc. Chem.* **30**(2), 571–573 (1993).
25. J. G. Young, W. Onyebuagu, "Synthesis and characterization of di-disubstituted phthalocyanines," *J. Org. Chem.* **55**(7), 2155–2159 (1990).
26. S. Kudrevich, N. Brasseur, C. LaMadeleine, S. Gilbert, J. E. vanLier, "Syntheses and photodynamic activities of novel trisulfonated zinc phthalocyanine derivatives," *J. Med. Chem.* **40**(24), 3897–3904 (1997).
27. K. J. M. Nolan, M. Hu, C. C. Leznoff, "Adjacent substituted phthalocyanines," *Synlett* **1977**(5), 593–594 (1977).
28. H. Ali, R. Langlois, J. R. Wagner, N. Brasseur, B. Paquette, J. E. van Lier, "Biological activities of phthalocyanines– X. Syntheses and analyses of sulfonated phthalocyanines," *Photochem. Photobiol.* **47**(5), 713–177 (1988).
29. J. Wang, H. Liu, J. P. Xue, Z. Jiang, N. S. Chen, J. L. Huang, "The constitutes and isomer distribution of di-(potassium sulfonate)-di-phthatimidomethyl phthalocyanine zinc," *Chin. Sci. Bull.* **53**(11), 1657–1664 (2008).
30. X. S. Li, N. Kwon, T. Guo, Z. Liu, J. Yoon, "Innovative Strategies for Hypoxic-Tumor Photodynamic Therapy," *Angew. Chem. Int. Ed.* **57**(36), 11522–11531 (2018).
31. H. Y. Ding, H. J. Yu, Y. Dong, R. H. Tian, G. Huang, D. A. Boothman, B. D. Sumer, J. M. Gao, "Photoactivation switch from type II to type I reactions by electron-rich micelles for improved photodynamic therapy of cancer cells under hypoxia," *J. Controlled Release* **156**(3), 276–280 (2011).
32. Z. Lv, H. J. Wei, Q. Li, X. L. Su, S. J. Liu, K. Y. Zhang, W. Lv, Q. Zhao, X. H. Li, W. Huang, "Achieving efficient photodynamic therapy under both normoxia and hypoxia using cyclometalated Ru(II) photosensitizer through type I photochemical process," *Chem. Sci.* **9**(2), 502–512 (2018).
33. J. S. Dysart, M. S. Patterson, "Characterization of Photofrin photobleaching for singlet oxygen dose estimation during photodynamic therapy of MLL cells in vitro," *Phys. Med. Biol.* **50**(11), 2597–2616 (2005).
34. J. Moan, K. Berg, E. Kvam, A. Western, Z. Malik, A. Ruck, H. Schneckenburger, "Intracellular localization of photosensitizers," *Ciba Found. Symp.* **146**, 95–107 (1989).
35. J. W. Shao, J. P. Xue, Y. C. Dai, H. Liu, N. S. Chen, L. Jia, J. L. Huang, "Inhibition of human hepatocellular carcinoma HepG2 by phthalocyanine photosensitiser Photocyanine: ROS production, apoptosis, cell cycle arrest," *Eur. J. Cancer* **48**(13), 2086–2096 (2012).
36. J. W. Shao, Y. C. Dai, W. N. Zhao, J. J. Xie, J. P. Xue, J. H. Ye, L. Jia, "Intracellular distribution and mechanisms of actions of photosensitizer Zinc(II)-phthalocyanine solubilized in Cremophor EL against human hepatocellular carcinoma HepG2 cells," *Cancer Lett.* **330**(1), 49–56 (2013).
37. A. P. Castano, T. N. Demidova, M. R. Hamblin, Mechanisms in photodynamic therapy: "Part three-Photosensitizer pharmacokinetics, biodistribution, tumor localization and modes of tumor destruction," *Photodiagn. Photodyn. Ther.* **2**(2), 91–106 (2005).
38. D. E. Dolmans, D. Fukumura, R. K. Jain, "Photodynamic therapy for cancer," *Nat. Rev. Cancer* **3**(5), 380–387 (2003).
39. B. W. Pogue, J. A. O'Hara, E. Demidenko, C. M. Wilmot, I. A. Goodwin, B. Chen, H. M. Swartz, T. Hasan, "Photodynamic therapy with verteporfin in the radiation-induced fibrosarcoma-1 tumor causes enhanced radiation sensitivity," *Cancer Res.* **63**(5), 1025–1033 (2003).
40. W. Liu, N. Chen, H. Jin, J. Huang, J. Wei, J. Bao, C. Li, Y. Liu, X. Li, A. Wang, "Intravenous repeated-dose toxicity study of ZnPcS2P2-based-photodynamic therapy in beagle dogs," *Regul. Toxicol. Pharmacol.* **47**(3), 221–231 (2007).